SOME SYSTEMATICS IN ELECTRON SCATTERING CROSS SECTIONS

GRZEGORZ KARWASZ and KAMIL FEDUS*

Nicolaus Copernicus University, Institute of Physics
Grudziadzka 5/7, 87-100 Torun, Poland

Received November 30, 2012
Accepted for Publication January 30, 2013

Operation of thermonuclear reactors will require knowledge of numerous cross sections for electron interaction with atoms and molecules, largely unknown at present and difficult for experiments. Theory is needed, but first it has to be verified on laboratory-accessible targets. A few working hypotheses and systematic approaches for various electron scattering processes are recommended. We discuss briefly analogies between total cross sections for scattering on nonpolar (BF_3, CO_2), polar (H_2O, NH_3, PF_3), reactive (BCl_3, HCl), and hexafluoride (SF_6, WF_6) molecules. For partial cross sections (ionization, elastic, electronic excitation), we search for some partitioning schemes. Similarly, we treat the vibrational excitation at shape resonances in linear triatomic molecules (N_2O, CO_2, OCS). Electron attachment for targets such as CCl_4 or CF_3I rises quickly toward the zero-energy limit; semiempirical approaches fail, but new theories work well. The paper, in general, shows ways to multitask construction of cross sections rarely measured in laboratories.

KEYWORDS: *electron scattering cross section, electron attachment*

Note: The figures in this paper are in color only in the electronic version.

I. INTRODUCTION

The extent of new problems for controlled thermonuclear fusion requires, among other things, detailed information on low-temperature plasma processes. Apart from deuterium[1] and helium, other targets for which cross sections are needed have rarely been studied in electron collision experiments. These targets comprise metals, such as Be, Cu, Cr, and Zr (Ref. 2) together with W, their hydrides, metal-substituted hydrocarbons, etc. The theory produces valuable results for light metals (e.g., Ref. 3), but it is difficult to verify theoretical models when no experiments exist, especially for heavy metals[4] and related molecules.

In this paper we quote some benchmark reviews, some series of experiments, and some promising theories for electron scattering on atoms and molecules. We also reviewed some possible semiempirical and comparative methods to predict total and partial cross sections for processes such as vibrational excitation, ionization, and electron attachment (EA). This overview does not give directly cross sections for the targets involved in the planned fusion reactors but, we hope, should stimulate comparative predictions and new experiments and theories.

II. EXPERIMENTAL TECHNIQUES AND CROSS-SECTION DATABASES

Since the 1960s, numerous databases for experimental electron scattering have been collected. From today's perspective, a great number of the early works are still valid. Examples are early swarm measurements to derive momentum transfer cross sections in polar molecules such as NH_3 (Ref. 5) or the cyclotron resonance technique used for the same molecules by Tice and Kievelson.[6] The early transmission measurements of Ramsauer and Kollath[7] for a long time were the only available total cross sections (TCSs) in N_2O below 1 eV, and only in the 1980s were these results confirmed by more advanced experiments. This is not the case for the measurements of TCSs by Brode[8] for targets such as Na, K, and other metals, which are not in agreement with more recent

*E-mail: kamil@fizyka.umk.pl

measurements from researchers at Wayne State University in Detroit, Michigan.[9] However, this more recent experiment also was not free of drawbacks; in the limit of low energy, the TCS could be underestimated because of the angular resolution error, due to the use of a high magnetic field guiding electrons through the scattering cell (e.g., Ref. 10).

For some targets an interactive synergy between the theory, semitheoretical approaches, and ab initio calculations recently allowed production of congruent sets of cross sections. For example, this is the case for nitric oxide (see Fig. 1), NO, which is an open-shell system and thus was tedious for the theory. The characteristic resonant structure in the NO cross section known from the early vibrational excitation measurements[11] and from theory[12] was found also in the TCS in the 1990s by Alle et al.[13] The latter measurement together with swarm data[14] triggered a semiempirical analysis in search of resonance vibrational excitations,[15] which were then confirmed by precise measurements[16]; those in turn triggered ab initio theory.[17] The semiempirical data[15] have been used successfully to model the infrared NO emissions in polar auroras.[18] A characteristic feature of the cross sections in NO is a high contribution of resonant vibrational excitations (see Fig. 1), which significantly influences the low-temperature electron drift coefficients.[14]

Very few experiments have been performed for metals. The early results of the recoil beam experiment by Kasdan et al.[19] still remain unique at low energies (~1 eV) for targets such as Li and Na and their halides and dimers (see paragraphs 3.1 and 3.2 in Ref. 20). For alkali metals those data indicate a monotonic fall of the TCS in the 1- to 100-eV range, with cross-section values of $\sim 200 \times 10^{-20}$ m^2 for Li and Na and 250×10^{-20} to 300×10^{-20} m^2 for K, Rb, and Cs (see Ref. 20). Theories predict somewhat more complicated dependencies of the TCS on energy, including some low-energy minima in Cs, which need to be verified. For Hg a maximum of the TCS of $\sim 250 \times 10^{-20}$ m^2 at 0.5 eV is predicted from (rather old) swarm data (see Ref. 20).

Worth remembering is the method proposed by Fermi for determining the zero-energy cross sections for atoms; such data would be useful as a cross-check for theories and results of swarm experiments. The method consists of studies of broadening of the atomic emission lines in the presence of some perturbing molecules (see, for example, Ref. 21 for data on Hg). Now the method is used sporadically,[22] and researchers hesitate to derive cross sections from the experiment.

The databases for electron scattering are usually collected by national institutions [for example, the French Gaphyor system, Japan's National Institute for Fusion Science (NIFS), and Korea's National Fusion Research Institute], but earlier efforts were undertaken by individual researchers: The files of JILA at the University of Colorado at Boulder were maintained by Phelps,[23] Hayashi published extensive, separate bibliographies for many gases,[24] and so on. A critical approach is quite often necessary—several gases in Phelps's compilations bear labels: "These data need urgently an upgrade."

A great effort to deliver recommended cross sections for targets of interest to the semiconductor industry such as CF_4 (Ref. 25), C_2F_6, C_3F_8, and SF_6 was done by Christophorou and collaborators at the National Institute of Standards and Technology (NIST) in Gaithersburg, Maryland. Extensive sets of cross sections for targets of atmospheric interest such as H_2, N_2 (Ref. 26), O_2, and H_2O

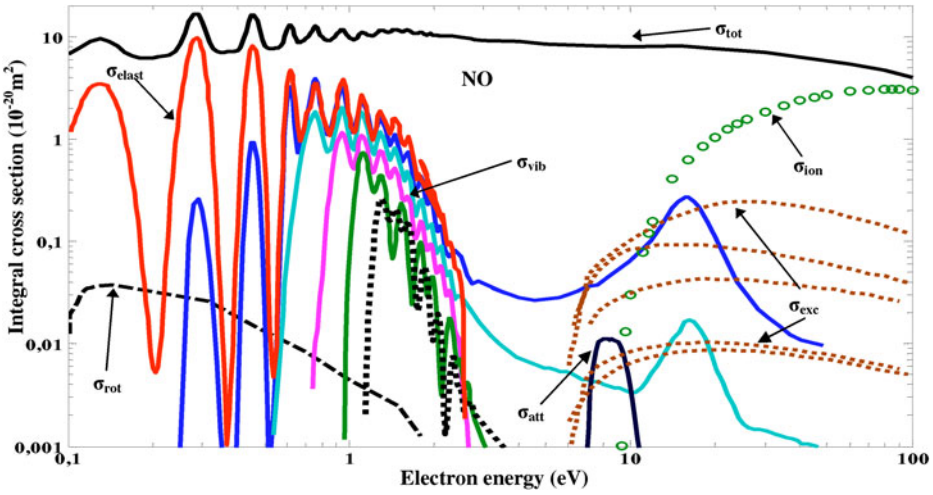

Fig. 1. Nitric oxide (NO) is one of the few targets for which cross sections for partial processes (rotational excitation, vibrational excitation, EA, electronic excitation, ionization) are relatively well-known. The most interesting feature, the progression of the vibrational modes in the low-energy resonance, has been recognized in a multistep interaction between the theories and experiments (see text for details).

were reported by Itikawa at NIFS. In our reviews,[20,27,28] total and partial cross sections of some 70 gases starting from atomic hydrogen and helium up to WF_6 were analyzed. We quoted extensive collections of papers but reviewed them laconically, not giving recommended but rather "preferred" experimental cross sections for partial processes, in order to compare their sum with the TCS. Those reviews also recall some open questions on simple theories, such as the convergence of atomic differential cross sections in the high-energy (Born) limit, the energy dependence of scattering amplitude phase shifts for noble gases at low energies, the dependence of TCSs for alkali-metal halides on their dipole moment and on the polarizability for alkali-metal dimers, the electronic excitation of optically forbidden states (leading to molecular dissociation), and so on.

In this paper we compare targets that are rarely presented in reviews but could serve as some analogies to predict cross sections in targets needed for modeling the thermonuclear reactors. We start from the TCSs, which allows a normalization of other data—elastic, vibrational—both differential and integral. Some search for analogies in total and partial cross sections follows in the second part of the paper. For the sake of data quality evaluation, we also discuss some possible errors in experiments, where it can be clarified.

III. TOTAL CROSS SECTIONS

The TCS σ_t describes the overall probability of scattering. In the optical theorem[29] this would be a kind of "invariant" for a given target, according to Eq. (1):

$$\mathrm{Re}[\,f(0,E)] = f_B(0,E) - g_B(0,E) + \frac{k}{4\pi^2}\int_E^\infty \frac{\sigma_t}{E'-E}\,\mathrm{d}E' \quad , \qquad (1)$$

where

f = scattering amplitude at zero angle

f_B = scattering amplitude in the Born approximation

g_B = exchange scattering amplitude

E, k = energy and wave number of the scattered electron, respectively.

Following this equation, the integral of the TCS from zero energy to infinity depends only on the zero-energy scattering amplitude. Kauppila and collaborators[30] tried in the 1970s to verify it, but the data were missing, in both the zero-energy as well as the high-energy limits. The TCS in a wide energy range could be key information to electron scattering properties of atoms or molecules.

Experiments using photoelectrons from synchrotron radiation sources by Jones et al.[31] and Kitajima et al.[32] allowed us to lower the energy range of the TCS down to some tens of milli-electron-volts. Swarm experiments, especially in noble gases with some molecular additives, remain a sensible tool for determining both elastic and inelastic (mainly vibrational) cross sections (see Nakamura, "Electron Swarm Parameters and Electron Collision Cross Sections," in this issue). Combining measurements with theories extending to zero energy and some high-energy extrapolations should allow us to use/verify the dispersion relation, Eq. (1). Unfortunately, the TCS is known in a wide energy range only for a few targets.

In Fig. 2 we show such data[33] for CO_2, which is a nonpolar molecule but shows a rise of the TCS in the zero-energy limit. This feature is frequently attributed to so-called virtual resonance, but it can be reproduced[34] via the modified effective range theory (MERT) using essentially only two scattering potentials, short range and polarization.

Recent theories (e.g., Ref. 35 for BF_3) yield quite reliable elastic cross sections, especially at low energies (below tens of electron-volts) where the elastic scattering constitutes the main part of the TCS. The theoretical shape resonances at low energies[35] are usually narrower and higher than the experimental TCS (Ref. 36) (see Fig. 2 for BF_3), probably because of disregarding the nuclear motion in the calculation. This discrepancy should not affect plasma modeling much.

The TCS can be measured relatively easily with a few percent precision. Higher errors, difficult to predict,

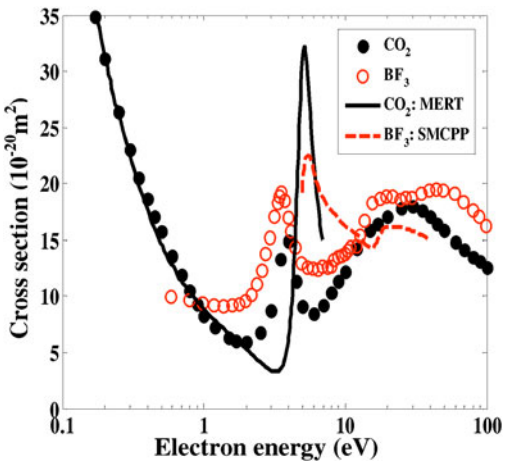

Fig. 2. Theory versus experiment: Theoretical predictions of shape resonances in small, nonpolar molecules. Both theories presented here overestimate the elastic cross section (both are fixed frame); they also overestimate the position of the resonance, probably because of the underestimation of the scattering potential (for MERT, no quadrupole moment is included). The experimental TCSs are CO_2 from the Landolt-Börnstein database[33] and BF_3 from Szmytkowski et al.[36] The theoretical lines correspond to elastic scattering: MERT for CO_2 (Ref. 34) and the Schwinger multichannel method with pseudopotentials (SMCPP) for BF_3 (Ref. 35).

occur in the case of forward-centered scattering, i.e., at high energies, especially in the presence of optically allowed electronic excitations. For the high-energy range (above 1000 eV), the TCSs of Garcia and Manero[37] and of Ariyasinghe and collaborators[38] are recommended.

The measured TCS in the case of polar targets can suffer from the angular resolution underestimation also at low energies—the experiments hardly discriminate against rotational excitations of the molecule, which are forward centered. As a consequence, the TCS in polar molecules, H_2O (Ref. 33), NH_3 (Refs. 31 and 39), and PF_3 (Ref. 36), rises rapidly in the zero-energy limit (see Fig. 3). Another source of the TCS underestimation is the use of a guiding magnetic field and large apertures in the scattering cell,[40] which is probably the case for the TCS measurements in HCl (see Fig. 4). Recent measurements performed with low magnetic field and good angular resolution[31] indicate for all polar molecules a rapid rise of the TCS in the zero-energy limit, up to $\sim 2000 \times 10^{-20}$ m^2 at 30 meV in H_2O and 900×10^{-20} m^2 at the same energy in NH_3.

The shape of the TCS in PF_3 resembles those in NH_3 and H_2O but is higher in absolute values (see Fig. 3). Also, the data by Szmytkowski and collaborators[36] rise quickly in the zero-energy limit—PF_3 is polar, like NH_3, but with lower (1.03D) dipole moment than NH_3 (1.47D), so the angular resolution underestimation in the experiment is probably smaller. Maxima in the TCSs for H_2O and NH_3 are due to several partially overlapping resonances that are better visible in vibrational excitation and dissociative attachment channels (e.g., Ref. 41).

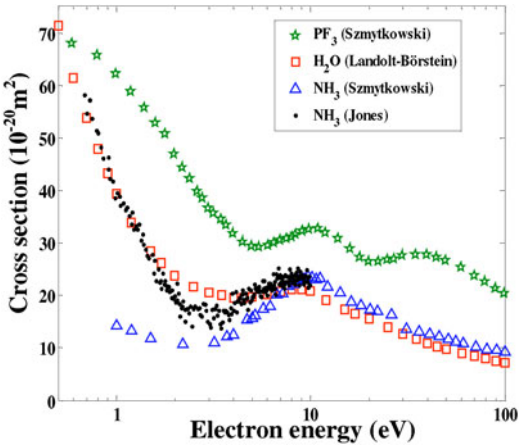

Fig. 3. Analogs in TCSs for polar molecules PF_3, H_2O, and NH_3. Data for PF_3 and H_2O are from measurements of Szmytkowski et al.[36] and Landolt-Börnstein database,[33] respectively. The experimental data of Szmytkowski et al.[39] for NH_3 in the zero-energy limit are much lower than the more recent measurements of Jones et al.,[31] because an angular resolution error is not excluded in Ref. 39.

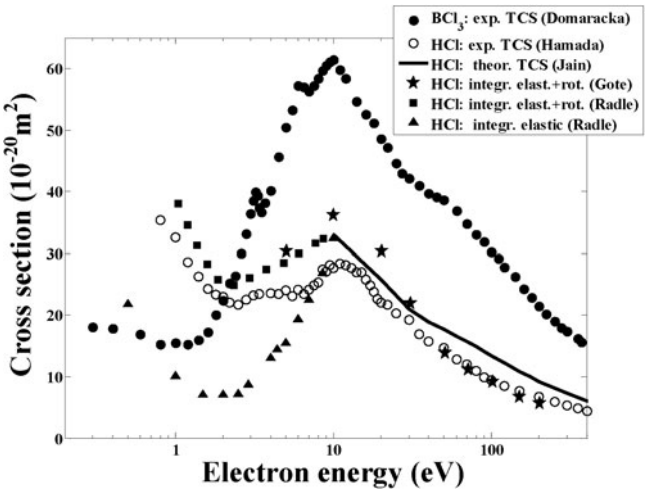

Fig. 4. Comparison of TCSs for chlorides: HCl (strongly polar) and BCl_3 (nonpolar). The TCS shows a maximum at $\sim$10 eV; a Ramsauer-Townsend minimum is visible in the TCS in BCl_3 and in HCl only in rotationally resolved elastic cross-section measurements (triangles, from Rädle et al.[45]). The experimental TCSs for BCl_3 and HCl are from Domaracka[42] and Hamada et al.,[43] respectively. The elastic + rotational cross sections for HCl are integrated from experimental differential cross sections of Gote et al.[44] and Rädle et al.[45] The theoretical TCS for HCl is from Jain et al.[46]

In Fig. 4 we compare the TCS in BCl_3 (nonpolar)[42] with the TCS and elastic integral (with the rotational excitation resolved) in HCl (Refs. 43 through 46). Both molecules show a broad maximum in the TCS at $\sim$10 eV, about twice higher in BCl_3 than in HCl, and Ramsauer minima at 1 to 2 eV. Between 1 and 10 eV BCl_3 shows some narrower peaks, probably due to resonant scattering. The theory (optical potential model) predicts[46] well the TCS at intermediate and high energies while the experimental TCS can be underestimated due to the normalization.[43]

In Fig. 5 we compare TCSs for tungsten and boron fluorides, WF_6 (Ref. 47) and BF_3 (Ref. 36) (and that for SF_6, recommended values from Ref. 33). At energies above 20 eV, TCSs scale with the summed atomic numbers of the molecules. For WF_6 the TCS in the whole energy range considered is almost exactly double that of BF_3, with shape resonances at $\sim$3 to 4 eV, the maximum value of the TCS at $\sim$50 eV, and a hump at $\sim$20 eV (probably due to dissociation into neutrals, in analogy with CF_4) for both molecules.

Figures 3, 4, and 5, chosen for chemical analogs, suggest that the TCS scales in some way with the summed atomic number and/or with the number of valence electrons and/or with the molecular polarizability. Such additivity rules have been hypothesized already by Brüche[48] and undertaken in many recent works. In Figs. 6 and 7 we

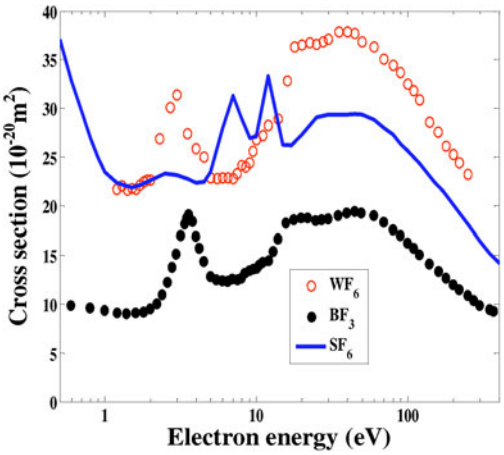

Fig. 5. Comparison of TCSs for nonpolar fluorides: e^--BF_3 scattering[36] (closed circles) and WF_6 (open circles)[47] and SF_6 (line, recommended values from Ref. 33). The cross section in WF_6 is almost exactly double that in BF_3 in the whole energy range compared.

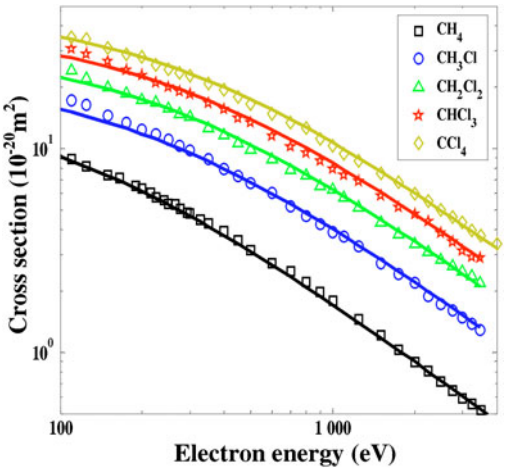

Fig. 7. Additivity rule applied to TCSs in halomethanes at high energies.[53] Having obtained scaling parameters for atoms, namely for H, C, Cl, and F from H_2, CH_4, CCl_4, and CF_4, the TCSs for all mixed compounds can be predicted.

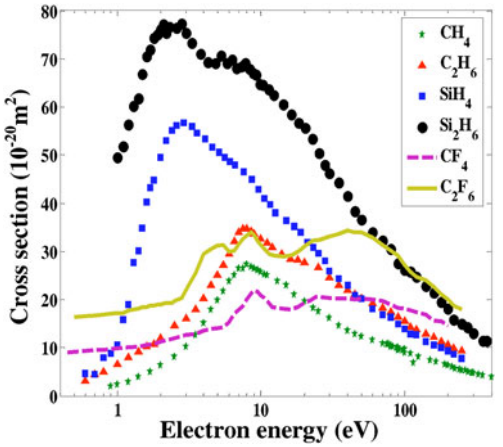

Fig. 6. TCSs for electron scattering on simple hydrocarbons, silanes, and fluorides: CH_4 (Ref. 49) versus C_2H_6 (Ref. 50), SiH_4 versus Si_2H_6 (Ref. 51), and CF_4 and C_2F_6 (Ref. 47). Note the essential similarities in the TCS curves—the amplitudes of the TCSs for a given central atom seem to scale with the number of "valence" atoms (H or F).

compare other pairs of chemical analogs: CH_4 versus C_2H_6 (Refs. 49 and 50), SiH_4 versus Si_2H_6 (Ref. 51), and CF_4 versus C_2F_6 (Ref. 47).

Some rough similarities clearly appear: The TCSs for a given chemical species seem to scale with the number of valence atoms, H or F. At the intermediate energy range, the TCSs descend smoothly with energy. García and Manero[37] related the TCS to the polarizability and the number of electrons in the target molecule; their semiempirical dependence of the TCS on energy $E^{-0.78}$ reproduces well experimental data but lacks any theoretical justification. The formula proposed by the author (G. K.) is based on the Born approximation for Yukawa potential[52] and the Thomas-Fermi model of the atom.[53] It reproduces well the TCS at high energies, as in Fig. 7 for halomethanes, but needs to be verified again, as the experimental data[52] were in error (by some 10% to 20%) in their high-energy limit, as explained before.

IV. PARTIAL CROSS SECTIONS

In plasma modeling it is not TCSs that predominantly influence plasma kinetics and chemistry but partial cross sections (electronic excitation, ionization, EA, etc.). TCSs can serve only as an indicator for amplitudes of partial processes.

Starting from the lowest energies, the rotational excitations do not change the energy balance in plasma much but do change the scattering angles of electrons. However, in mixed plasmas, as compared to plasmas containing only atomic species, and particularly in the presence of polar molecules, via their rotational excitations, the electron temperatures can change significantly. The experiments on rotational excitations were done only for a few molecules, such as HCl (Ref. 45) (see Fig. 4). In the previous review we compared the differential cross sections for $\Delta J = 0$, 1, 2 transitions for these molecules (see Figs. 10 and 11 in Ref. 27). Outside resonances, the rotational excitation can be estimated from Born's formula[54]:

$$\sigma_{rot}(J \to J \pm 1) = \frac{8\pi}{3k^2} D^2 \frac{J}{2J+1} \ln \frac{k+k'}{|k-k'|} , \quad (2)$$

where k and k' are initial and final wave numbers, respectively, and D stands for the permanent dipole moment of the molecule (in atomic units). Čurik et al.[55] recently developed a more precise theory that succeeded in the analysis of experimental TCSs in H_2O in the milli-electron-volt range; their results do not differ much from the Born formula.

Similarly, the Born approximation proved to be valid also for vibrational excitations:

$$\sigma_{vib}(v \to v') = \frac{8\pi}{3k^2}\, g' |\langle v'|D|v\rangle|^2 \ln \frac{k+k'}{|k-k'|} \quad . \qquad (3)$$

In this case the temporary dipole transition moment $\langle v'|D|v\rangle$, with v and v' indexing initial and final vibrational states, respectively, is the "driving force" of the excitation (g' stands for the degeneracy of the upper state). This relation has been verified recently even for positron scattering.[56] In a review (Fig. 13), we show that the vibrational excitation in CF_4 is so strong that it almost masks the presence of Ramsauer minimum in TCS. The vibrational excitation shows for some targets narrow peaks just above thresholds. In Ref. 27 we show it in HCl. Again, the presence of threshold peaks should not influence results of plasma modeling much.

Next on the energy scale among the scattering channels are electronic excitations, which may have quite low thresholds, like those for the optically forbidden states $a^1\Delta_g$ (0.98 eV) and $b\Sigma_g^+$ (1.63 eV) in O_2. For light targets the optically forbidden states[57] may have very long lifetimes (the $a^1\Delta_g$ state in oxygen is as long as ~75 min). Excitations to the forbidden states can also show resonant enhancements (see Fig. 28 in Ref. 27) for the $a^1\Delta_g$ state in O_2. At high energies cross sections fall quickly with energy, somewhat like E^{-3} or quicker (see Fig. 20 in Ref. 27 for the $b^3\Sigma_u^+$, $a^3\Sigma_g^+$, and $c^3\Pi_u$ states in H_2 molecule). In contrast, optically allowed electronic excitations change slowly with energy, with an energy dependence of the cross sections resembling those for vibrational excitations. The amplitudes of the electronic excitation integral cross sections can be predicted, to the first approximation, from the photoabsorption cross sections (for example, Ref. 58), which via the optical theorem correspond to the zero-angle differential cross sections for electronic excitation. The differential cross sections for optically allowed states are forward centered, but those for the optically forbidden states are difficult to predict even in targets such as N_2 (Ref. 59).

Very few measurements exist for dissociation into neutrals. This process is important in gases such as SiH_4 and CF_4 (see Figs. 12 and 13). For CF_4 the dissociation to neutrals (without forming ionized fragments) is significant at energies close to threshold, ~20 to 30 eV, where it can account for as much as 5% to 10% of the TCS (Ref. 28). For SiF_4 molecules the summed cross sections for different channels leading to dissociation into neutral fragments amount at 100 eV to half of the summed cross sections for ionization.[60] Dissociation into neutrals goes frequently via optically forbidden electronic excitations. Therefore, two types of measurements (electronic excitation and metastable fragments formation) are complementary; this is the case, for example, of the $c^3\Pi_u$ state in H_2 (Ref. 61).

The cross sections for molecular dissociation have been experimentally proved to follow some additivity rules. In CF_4 the cross section for the formation of the CF_3 radical is double those for the CF_2 or CF radical[62]—the F atom (or more probably the F^+ ion) can be detached from two distinguishable positions while the detachment of three F atoms is done in a single way. The "sum of reaction paths" is even better visible in CHF_3 molecules, where the cross section for CHF_2 formation is double that of the CF_3 formation and two-thirds that of the CF_3 radical formation cross section of the CF_4 molecule.[63]

Relatively well understood are the ionization processes, where the semiempirical approximation based on the binary encounter model predicts quite well both overall and partial ionization cross sections.[64] The values of the electron binding energies needed for the model can be calculated via quantum chemistry methods. The NIST database includes calculations of ionization cross sections for numerous targets in a friendly form.[65]

V. ELECTRON ATTACHMENT

Electron attachment is of special importance for plasmas since it quenches free electrons. In recent years significant progress has been made both in experiments as well as in the theory. Benchmark measurements of EA reaction constants for targets such as monohalobenzenes (C_6H_5I, C_6H_5Br, etc.) and pentafluorobenzenes (C_6F_5I, C_6F_5Br, etc.) were performed by the pulsed-radiolysis method by Shimamori and collaborators.[66] Another method yielding EA cross sections at sub-electron-volt energies is the Rydberg-atom (Rb, K) quenching developed by Dunning.[67]

The EA process can be classified into two mechanisms: (a) the near-to-zero-energy EA in targets such as SF_6 and CCl_4, where very high cross sections have been determined and parent anions are formed, and (b) the resonant electron capture, seen even in targets such as CH_4 in the region of the maximum of the TCS. The parent molecular ion (i.e., SF_6^- from SF_6) is formed when the excess energy available for the molecule after the EA can be dissipated via vibrational excitation.

In the zero-energy limit, the EA cross sections in targets with high electron affinity (such as SF_6, C_6F_6, CF_3I, and CCl_4) change as $E^{-3/4}$ (for example, between 0.1 and 10 meV in CF_3I). The following phenomenological fit was used, for example, by Marienfeld et al.[68] for CF_3I:

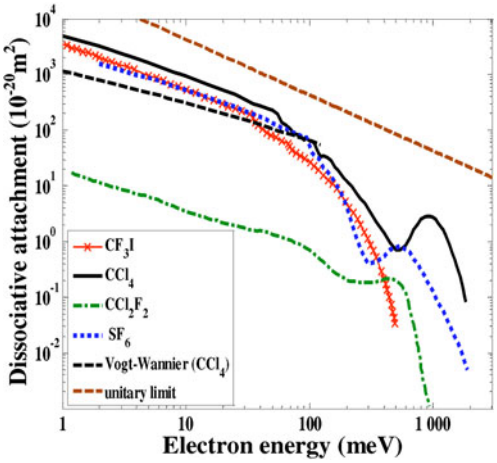

Fig. 8. Dissociative attachment cross sections for CF_3I, CCl_4, SF_6, and CCl_2F_2 in the zero-energy limit[68,69]; the Vogt-Wannier model[70] and the unitary limit π/k^2 are straight lines in this scale.

$$\sigma_A(E) = \frac{\sigma_0}{E}\left[1 - \exp(-\beta\sqrt{E})\right] , \qquad (4)$$

with $\sigma_0 = 5400$ Å^2 meV and $\beta = 0.93$ (meV)$^{-1/2}$.

For CCl_4 similar values of EA in the zero-energy limit were observed, $\sim 5.0 \times 10^{-17}$ m^2 at 1 meV (Ref. 69), while for SF_6 the EA is somewhat lower (less than by a factor of 2). This, according to the model of Vogt and Wannier,[70] reflects a lower polarizability of the latter molecule (6.5×10^{-30} m^3 for SF_6 and 10.8×10^{-30} m^3 for CCl_4). The experimental EA cross sections in the zero-energy limit are higher than those from the Vogt-Wannier model but lower than the unitary limit π/k^2 (see Fig. 8).

TABLE I

Energy-Integrated DEA Cross Sections

Model	Experiment
HCl 6.14×10^{-2} DCl 0.28×10^{-2}	6.85×10^{-2} 0.45×10^{-2}

*From Ref. 72; values in eV·Å^2.

The resonant EA scattering is much more difficult to model. Christophorou[71] indicated a semiempirical dependence, that the maximum of the resonant dissociative EA (DEA) cross section lowers with the rising energy of the resonance. He quoted targets such as CH_4, H_2O, and N_2O. More recent data (for example, Ref. 41) for H_2O only partially indicate similar dependence. Furthermore, a comparison for deuterated species[72] (see Table I) shows that the DEA cross sections depend much more on the molecular vibrations than on the position of the resonance. In fact, a strong temperature effect in DEA observed in HCl in the 1970s has only recently been explained by theory.[72]

Fabrikant[73] showed recently that the EA cross sections both at the zero-energy limit and at resonances can be derived once the energy potential curves are constructed (Fig. 9). His method, based on the *R*-matrix approach, needs some information from the experiment but proved to be quite successful for different types of molecules.[73]

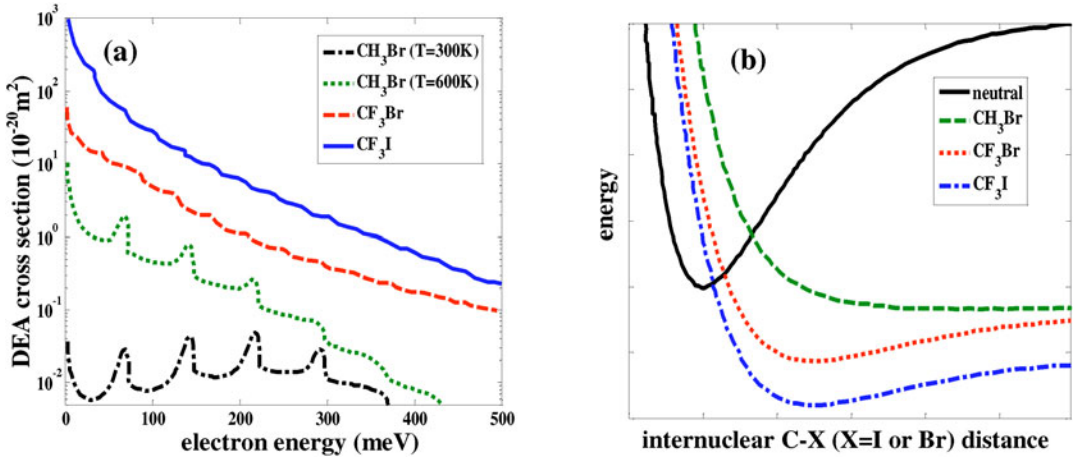

Fig. 9. (a) *R*-matrix calculations of DEA cross sections based on (b) the potential-energy curves of anions of three polar molecules (CH_3Br, CF_3Br, and CF_3I). In (a) the effect of temperature on the DEA for CH_3Br is also illustrated. In (b) the solid line represents a reference potential curve of the corresponding neutral molecule (M), while the broken curves are the potential curves for M-anions. Adapted from Ref. 73 with the author's permission.

VI. PARTITIONING SCHEMES

Determining single partial cross sections is one way of constructing sets of cross sections. Another, complementary method comes again from TCS analysis, by asking what is the relative contribution of every single channel to the TCS. The vibrational progression deduced for NO, Fig. 1, is an example of such a reasoning. Knowing the TCS as the upper limit for the sum and using the relative intensities between the elastic channel and vibrational overtones of the resonances in N_2 and CO (see Fig. 19 in Ref. 20), one predicts pretty well unknown cross sections for the vibrational excitation.

Constructing a partial cross section as a given part of the TCS may be useful in predicting, for example, electronic excitations. Theoretically, a correct prediction of the cross-section amplitude requires the calculation of oscillator strength; experimentally, the integral cross sections require tedious measurements of angular distribution of inelastically scattered electrons, then the extrapolation into the angles experimentally inaccessible and normalization of the gas flux. Possible errors, both in experiment and the theory, are big. On the other hand, the analysis of electronic cross sections in molecules such as H_2 or CH_4 shows that these cross sections do not exceed a few percent of the TCS. Therefore, some scaling is not much more imprecise than an experiment or theory.

Such an approach is shown in Fig. 10, where we compare elastic and ionization cross sections with the TCSs for three tetrahedral, spherical-like molecules, CH_4, SiH_4, and GeH_4, and their isoelectronic noble gas analogs, Ne, Ar, and Kr. First, note from Fig. 10 that the absolute values of elastic contributions to the TCSs are equal within the experimental error for the molecule–noble gas atom pairs (CH_4 versus Ne, etc.). Second, the ionization cross section is much higher in molecules than in noble gases. Third, the remaining part after the sum of the elastic and ionization cross sections (the upper part of the columns in Fig. 10) must account for all inelastic processes, including the electronic excitation and dissociation into neutrals. Again, cross sections for the latter two processes are higher in molecules than in noble gases.

A question arises of whether similar procedures can be tried at resonances. In Fig. 11 we compare TCSs in the region of the so-called shape resonances in three molecules with the same number of valence electrons. First, note that the maxima of the TCSs (solid, dotted, and dashed lines) scale as $1/k^2$ (dashed-dotted line), which was expected of EA in the limit of zero energy but not verified. On the same graph we show values of elastic cross sections (open symbols) and vibrational excitations (closed symbols). Within a very rough estimate (mainly due to the uncertainties in the experimental determination of the partial cross sections), the vibrational cross section in the TCS maximum is lower by a factor of ~2 than the elastic cross section. In other words, the vibrational excitation amounts to as much as one-third of the TCS. A similar analysis for the N_2 and CO analog pair indicated that at the low-energy resonance the vibrational excitation is roughly one-sixth of the TCS. The DEA at shape resonances shown in Fig. 11 is slightly less than 1% of the TCS (0.8% in NO_2 at 1.8 eV, 0.5% in OCS at 1.3 eV, 0.3% in N_2O at 2.2 eV, and 0.1% in CO_2 at 4.4 eV). In turn, in SF_6 in the limit of zero energy the EA constitutes as much as one-third of the TCS (Ref. 69).

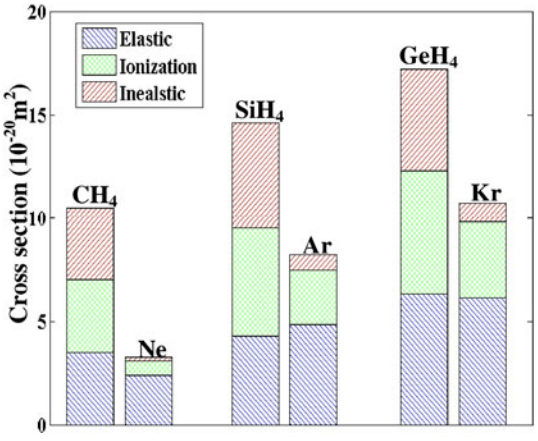

Fig. 10. Partitioning in noble gases versus isoelectronic spherical molecules; see Ref. 27 for the data used.

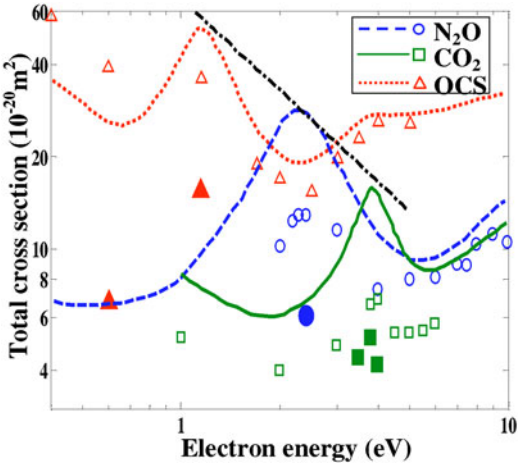

Fig. 11. Partitioning at shape resonances for valence-isoelectronic, linear triatomic molecules. Open symbols: elastic integral cross sections; closed symbols, vibrational excitation integral cross sections; dashed-dotted line, the $1/E$ dependence (E being energy); see Ref. 27 for the data used.

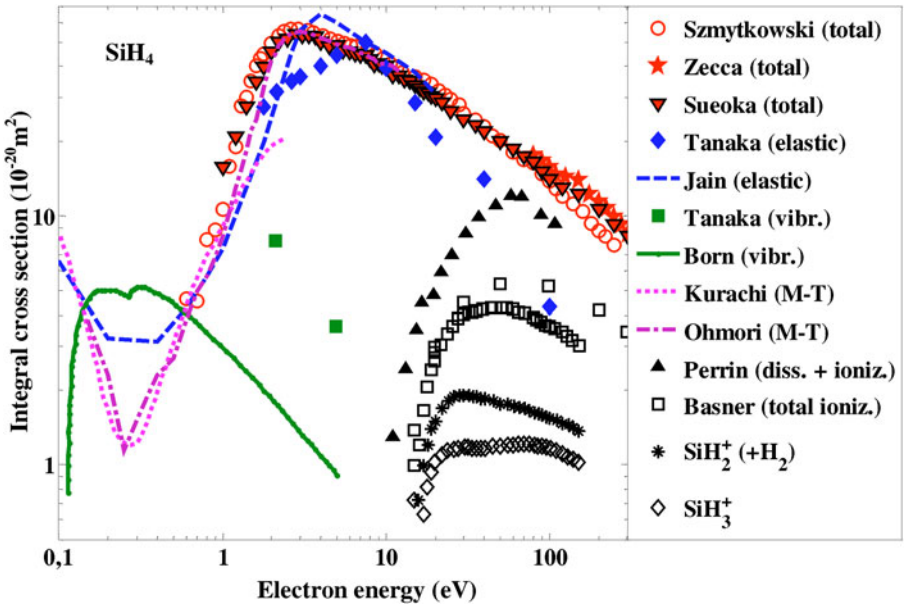

Fig. 12. Total, momentum transfer, and partial cross sections for electron scattering in silane. Ionization cross sections from Ref. 74 and dissociation convoluted data from Ref. 77; for the other sources see Ref. 27.

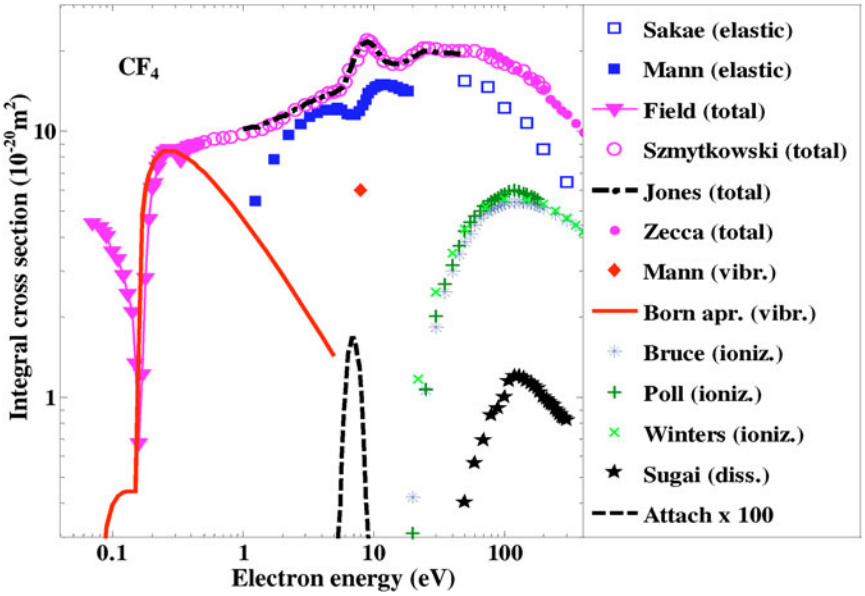

Fig. 13. Total and partial cross sections for electron scattering in tetrafluoromethane. Dissociation cross sections from Ref. 62; other details of the data sources are given in Ref. 28.

VII. CONCLUSIONS: CONSTRUCTION OF CROSS-SECTION DATA SETS

The TCSs, in principle, can be determined experimentally with a few percent precision; some bigger errors are possible at high energies and at low energies for polar molecules. Measurements using threshold electrons from the photoionization and the MERT allow us to extrapolate the TCSs down to thermal energies. Swarm measurements, in particular for mixtures such as SiH_4-Ar (Ref. 74), are an additional cross-check. Modern theories, such as the *R*-matrix[73] already mentioned or the

Schwinger variational approach,[72] produce reliable data for elastic, vibrational,[75] rotational, and EA cross sections but sometimes need scaling to the experiment.

Vibrational cross sections outside resonances can be found also from the Born approximation using dipole transition moments derived from photoabsorption measurements.[58] For resonances reliable models are still to be verified. Ionization cross sections can be determined fairly well at several laboratories and are predicted by semiempirical models.

Recent experiments delivered reliable ionization cross sections; see, for example, Ref. 76 for SiH_4. For the dissociation into neutrals (and determining energies and electronic states of the fragments), very few experiments exist[62,63] or they are indirect (via optical excitations) and so require some deconvolution, such as data for SiH_4 (Ref. 77). Also, experiments directly on plasmas (i.e., measurements of the electron density and temperature) yield information on the formation of radicals and reaction by-products, such as F_2 in CF_4 discharge.[78] In semiconductor industries[79] the low-energy dissociation of SiH_4 (and $SiCl_4$) is essential for production of Si nanocrystals by nonthermal plasmas,[80] but the relative cross sections are unknown.

All this knowledge is necessary for critical construction of the cross-section sets. Examples of cross-section sets constructed for the present work are shown in Figs. 12 and 13. At present, we do not know the cross sections in the low-energy limit for targets such as BeH_2, LiH, WH_4, etc. Chemical similarities can act as guidelines. Linking TCS dependences to some atomic/molecular features, such as polarizability, number of valence electrons, or hard-sphere radii (in MERT) would be valuable. Better understanding of partial processes in resonances is required. A multitasking effort combining theories and extending the range of experimental techniques in use (plasma, swarm, cyclotron resonance, recoil beam, Fermi method, etc.) is needed.

REFERENCES

1. J. S. YOON et al., *Rep. Prog. Phys*., **73**, 116401 (2010).

2. B. Y. KIM et al., *Fusion Sci. Technol*., **62**, 21 (2012).

3. O. ZATSARINNY et al., *J. Phys.: Conf. Ser*., **194**, 042029 (2009).

4. A. Z. MSEZANE et al., *J. Phys.: Conf. Ser*., **388**, 042002 (2012).

5. J. L. PACK et al., *Phys. Rev*., **127**, 2084 (1962).

6. R. TICE and KIEVELSON, *J. Chem. Phys*., **46**, 4748 (1967).

7. C. RAMSAUER and KOLLATH, *Ann. Phys*., **7**, 176 (1930).

8. R. B. BRODE, *Phys. Rev*., **34**, 673 (1929).

9. S. P. PARIKH et al., *Phys. Rev. A*, **47**, 1535 (1993).

10. G. P. KARWASZ et al., *Nucl. Instrum. Methods B*, **266**, 471 (2008).

11. R. AZRIA et al., *Phys. Rev. A*, **11**, 1309 (1975).

12. D. TEILLET-BILLY et al., *J. Phys. B*, **10**, L111 (1977).

13. D. T. ALLE et al., *J. Phys. B: At. Mol. Opt. Phys*., **29**, L277 (1996).

14. J. MECHLINSKA-DREWKO et al., *J. Phys. D*, **32**, 2746 (1999).

15. L. JOSIC et al., *Chem. Phys. Lett*., **350**, 318 (2001).

16. M. JELISAVCIC et al., *Phys. Rev. Lett*., **90**, 203201 (2003).

17. Z. ZHANG et al., *Phys. Rev. A*, **69**, 062711 (2004).

18. L. CAMBELL et al., *Geophys. Res. Lett*., **34**, L22102 (2007).

19. A. KASDAN et al., *Phys. Rev. A*, **8**, 1562 (1973).

20. A. ZECCA et al., *La Rivista del Nuovo Cimento*, **19**, *5* (1996).

21. R. S. TRAWINSKI, *Acta. Phys. Pol. A*, **110**, 51 (2006).

22. U. ASAF et al., *Phys. Rev. A*, **40**, 5458 (1989).

23. A. V. PHELPS, "Compilation of Electron Cross Sections Used by A. V. Phelps," JILA Web Site: http://jila.colorado.edu/~avp/collision_data/electronneutral/ELECTRON.TXT (current as of Nov. 30, 2012).

24. M. HAYASHI, "Bibliography of Electron and Photon Cross Sections with Atoms and Molecules Published in the 20th Century—Nitrogen Molecule," NIFS-DATA-77, National Institute for Fusion Science, Japan (June 2003).

25. L. G. CHRISTOPHOROU et al., *J. Phys. Chem. Ref. Data*, **28**, 4 (1999).

26. Y. ITIKAWA, *J. Phys. Chem. Ref. Data*, **35**, *1* (2006).

27. G. P. KARWASZ et al., *La Rivista del Nuovo Cimento*, **24**, *1* (2001).

28. G. P. KARWASZ et al., *La Rivista del Nuovo Cimento* **24**, *4* (2001).

29. F. J. HEER et al., *J. Phys. B*, **10**, 1945 (1977).

30. W. E. KAUPPILA et al., *Rev. Sci. Instrum*., **48**, 822 (1977).

31. N. C. JONES et al., *Phys. Rev. A*, **78**, 042714 (2008).

32. M. KITAJIMA et al., *Eur. Phys. J. D*, **66**, 130 (2012).

33. G. P. KARWASZ et al., "Electron Scattering with Molecules," *Photon and Electron Interaction, with Atoms, Molecules and Ions*, Vol. I/17, Chap. VI.1, p. 6.1, Landolt-Börnstein New Series, Springer-Verlag, Berlin (2003).

34. Z. IDZIASZEK et al., *J. Phys.: Conf. Ser.*, **115**, 012002 (2008).

35. R. F. DA COSTA et al., *J. Chem. Phys.*, **118**, 75 (2003).

36. C. SZMYTKOWSKI et al., *J. Chem. Phys.*, **121**, 1790 (2004).

37. G. GARCIA and MANERO, *Phys. Rev. A*, **57**, 1069 (1998).

38. W. M. ARIYASINGHE et al., *Nucl. Instrum. Methods B*, **217**, 389 (2004).

39. C. SZMYTKOWSKI et al., *J. Phys. B*, **22**, 525 (1989).

40. G. P. KARWASZ et al., *Nucl. Instrum. Methods B*, **247**, 68 (2006).

41. P. RAWAT et al., *J. Phys. B: At. Mol. Opt. Phys.*, **40**, 4625 (2007).

42. A. DOMARACKA et al., *Phys. Rev. A*, **71**, 052711 (2005).

43. A. HAMADA et al., *J. Phys. B*, **27**, 5055 (1994).

44. M. GOTE et al., *J. Phys. B*, **28**, 3957 (1995).

45. M. RADLE et al., *J. Phys. B*, **22**, 1455 (1989).

46. A. JAIN et al., *Phys. Rev. A*, **45**, 202 (1992).

47. C. SZMYTKOWSKI et al., *J. Phys. B: At. Mol. Opt. Phys.*, **33**, 15 (2000).

48. E. BRUCHE, *Ann. Phys. (Leipzig)*, **83**, 1065 (1927).

49. A. ZEECCA et al., *J. Phys. B: At. Mol. Opt. Phys.*, **24**, 2747 (1991).

50. C. SZMYTKOWSKI et al., *J. Phys. B: At. Mol. Opt. Phys.*, **34**, 605 (2001).

51. C. SZMYTKOWSKI et al., *J. Phys. B: At. Mol. Opt. Phys.*, **28**, 4291 (1995).

52. G. P. KARWASZ et al., *Phys. Rev. A*, **59**, 1341 (1999).

53. G. P. KARWASZ et al., *Phys. Rev. A*, **61**, 024701 (2000).

54. Y. ITIKAWA, *J. Phys. Soc. Jpn.*, **36**, 1127 (1974).

55. R. CURIK et al., *Phys. Rev. Lett.*, **97**, 123202 (2006).

56. T. NISHIMURA et al., *Nucl. Instrum. Methods B*, **192**, 17 (2002).

57. M. A. KHAKOO et al., *J. Phys. B*, **16**, L317 (1983).

58. W. F. CHAN et al., *Chem. Phys.*, **180**, 77 (1994).

59. I. LINERT et al., *J. Phys. B: At. Mol. Opt. Phys.*, **42**, 8 (2009).

60. R. BASNER et al., *J. Chem. Phys.*, **114**, 1170 (2001).

61. N. J. MASON et al., *J. Phys. B*, **19**, L587 (1986).

62. T. NAKANO et al., *Jpn. J. Appl. Phys.*, **31**, 2919 (1992).

63. S. MOTLAGH et al., *J. Chem. Phys.*, **109**, 432 (1988).

64. Y. K. KIM et al., *Phys. Rev. A*, **50**, 3954 (1994).

65. Y. K. KIM et al., "Electron-Impact Cross Sections for Ionization and Excitation," National Institute of Science and Technology Web Site: http://physics.nist.gov/PhysRefData/Ionization/Xsection.html (current as of Nov. 30, 2012).

66. H. SHIMAMORI et al., *Chem. Phys. Lett.*, **232**, 115 (1995).

67. F. B. DUNNING, *J. Phys. Chem.*, **91**, 2244 (1987).

68. S. MARIENFELD et al., *J. Phys. B: At. Mol. Opt. Phys.*, **39**, 105 (2006).

69. M. BRAUN et al., *J. Phys. B: At. Mol. Opt. Phys.*, **42**, 125202 (2009).

70. E. VOGT and WANNIER, *Phys. Rev. A*, **95**, 1190 (1954).

71. L. CHRISTOPHOROU, in *Gaseous Dielectrics III: Proc. Third Int. Symp. Gaseous Dielectrics*, Knoxville, Tennessee, March 7–11, 1982.

72. J. FEDOR et al., *J. Phys.: Conf. Ser.*, **194**, 052036 (2009).

73. I. I. FABRIKANT, *J. Phys.: Conf. Ser.*, **192**, 012002 (2009).

74. M. KURACHI et al., *J. Phys. D: Appl. Phys.*, **21**, 602 (1988).

75. J. FRANZ et al., *Phys. Rev. A*, **80**, 012709 (2009).

76. R. BASNER et al., *Int. J. Mass Spectrom. Ion Processes*, **171**, 83 (1997).

77. J. PERRIN et al., *Chem. Phys.*, **80**, 351 (1983).

78. S. X. ZHAO et al., *Plasma Sources Sci. Technol.*, **21**, 025008 (2012).

79. D. R. COTE et al., *IMB J. Res. Develop.*, **43**, 1/2 (1999)

80. R. GRESBACK et al., *Nanotechnology*, **22**, 305605 (2011).